

Article

# Electrochemical Activation and Its Prolonged Effect on the Durability of Bimetallic Pt-Based Electrocatalysts for PEMFCs

Angelina Pavlets <sup>1</sup>, Ilya Pankov <sup>2</sup>  and Anastasia Alekseenko <sup>1,\*</sup> <sup>1</sup> Faculty of Chemistry, Southern Federal University, 7 Zorge St., Rostov-on-Don 344090, Russia<sup>2</sup> Research Institute of Physical Organic Chemistry, Southern Federal University, 194/2 Stachki St., Rostov-on-Don 344090, Russia

\* Correspondence: an-an-alekseenko@yandex.ru

**Abstract:** The present study, concerned with high-performance ORR catalysts, may be a valuable resource for a wide range of researchers within the fields of nanomaterials, electrocatalysis, and hydrogen energy. The objects of the research are electrocatalysts based on platinum–copper nanoparticles with onion-like and solid-solution structures. To evaluate the functional characteristics of the catalysts, the XRD, XRF, TEM, HAADF-STEM, and EDX methods, as well as the voltammetry method on a rotating disk electrode have been used. This work draws the attention of researchers to the significance of applying a protocol of electrochemically activating bimetallic catalysts in terms of the study of their functional characteristics on the rotating disk electrode. The choice of the potential range during the pre-cycling stage has been shown to play a crucial role in maintaining the durability of the catalysts. The activation of the PtCu/C catalyst during cycling of up to 1.0 V allows for an increase in the durability of the catalysts with onion-like and solid-solution structures of nanoparticles by 28% and 23%, respectively, as compared with activation of up to 1.2 V.

**Keywords:** electrocatalysts; ORR; PEMFCs; Pt-based; nanoparticles; durability



**Citation:** Pavlets, A.; Pankov, I.; Alekseenko, A. Electrochemical Activation and Its Prolonged Effect on the Durability of Bimetallic Pt-Based Electrocatalysts for PEMFCs. *Inorganics* **2023**, *11*, 45. <https://doi.org/10.3390/inorganics11010045>

Academic Editors: Qinggang He, Shaowei Chen and Zidong Wei

Received: 29 November 2022

Revised: 17 December 2022

Accepted: 30 December 2022

Published: 16 January 2023



**Copyright:** © 2023 by the authors. Licensee MDPI, Basel, Switzerland. This article is an open access article distributed under the terms and conditions of the Creative Commons Attribution (CC BY) license (<https://creativecommons.org/licenses/by/4.0/>).

## 1. Introduction

Pt-based electrocatalysts are the main components of membrane electrode assemblies (MEAs) for proton-exchange membrane fuel cells (PEMFCs) [1,2]. Alloying the platinum with d-metals allows for both the enhancement of the performance of the electrocatalysts and a decrease in the loading of the precious metal, thus lowering its cost [3]. The positive effects of alloying platinum with other metals, including Ni, Co, Cu, Fe, etc., have been well-established in a substantial number of publications [4–7].

The current works in the field of studying the bimetallic catalysts for PEMFCs are aimed at obtaining materials based on PtM nanoparticles (NPs) with differing architectures (core–shell, gradient, solid solution, nanowire, and nanoframe), which may provide higher levels of activity in the oxygen reduction reaction (ORR) [5,6,8–13]. To a lesser extent, these studies are aimed at scaling the methods to obtain these catalysts [14,15]. Conversely, the question relating to the processes of the NPs' evolution during the operation of the catalysts remains less studied [16–20].

It is known that, in order to be used in PEMFCs, PtM/C catalysts must undergo a special treatment such that the “de-alloyed” structure of NPs, which would not subject to the selective dissolution of the d-metal during the operation, might be obtained [21]. The de-alloyed materials are obtained by chemical (acid treatment) [22–24] and electrochemical (potential hold and voltametric cycling) methods [25–28]. The acid treatment is promising for scaling and the commercial production of de-alloyed catalysts due to the fact that large quantities of the product can be processed simultaneously, and this processing is easily achieved via the equipment and reagents used. However, based on the literature data, it can be concluded that the electrochemical methods allow for the obtaining of the

catalysts with much higher activity in the ORR. So far, there have been few studies on the results of the effect of the electrochemical activation conditions on the characteristics of the obtained materials.

It is assumed that the detailed analysis of the evolution of the catalytic behavior as a result of electrochemical treatments under different conditions should be conducted. This approach would allow for the further design and prediction of methods to obtain highly active catalysts with a stable, de-alloyed structure.

Along with the ORR activity, the durability of the materials during accelerated degradation testing (ADT) needs studying. During these measurements, the degradation of the catalysts is observed. The degradation is registered with regard to the decrease in the functional characteristics, i.e., the electrochemical surface area (ESA) and the ORR activity [29–31].

Previous studies have shown that the potential window during the activation stage has a significant impact on the ORR activity of the obtained de-alloyed materials [18,32]. The novelty of this study is due to the establishment of the correlation between the electrochemical activation protocol and the durability of the PtCu/C catalysts. The promising catalysts, which are based on NPs with onion-like and solid-solution structures, have been chosen as the research samples. A specific feature of this work is its analysis of the characteristics of the catalysts obtained by the gram-scale synthesis method. This study is of applied interest in the field of the production of the highly active and stable nanostructured catalysts for hydrogen energy.

## 2. Results and Discussion

Two types of catalysts were prepared via liquid-phase synthesis. The S1 sample was synthesized in one stage via the coreduction of the copper and platinum precursors in order to obtain NPs with a solid-solution structure [19].

The S2 sample was synthesized according to a patented technique (patent No. RU2778126C1), which consists of the preliminary preparation of the Pt/C material with a uniform distribution of Pt NPs over the support surface [13]. The metals' precursors were then deposited on these particles in three stages such that the onion-like structure of the NPs would be formed, with the Pt-enriched layers being located on the surface of this structure.

The obtained catalysts are characterized by a closed mass fraction of the metals and platinum (Table 1). The composition of the metal components, as determined by the XRF method, is close to a ratio of Pt:Cu = 1:1 for both of the catalysts (Table 1).

**Table 1.** The compositional characteristics of the PtCu/C catalysts.

| Sample | Mass Fraction of Pt, % | Mass Fraction of Metal, % | Atomic Composition (XRF)          |
|--------|------------------------|---------------------------|-----------------------------------|
| S1     | 19.0                   | 27.1                      | Pt <sub>43</sub> Cu <sub>57</sub> |
| S2     | 20.4                   | 25.1                      | Pt <sub>56</sub> Cu <sub>44</sub> |

The XRD patterns of the obtained PtCu/C materials are presented in Figure S1. The X-ray diffraction patterns have the typical appearance of bimetallic Pt-based catalysts with a carbon support [33,34]. The reflection maximum of the (111) facet is shifted to the high-angle region of  $2\theta$ , as compared with pure platinum. This testifies to the alloying of the metal components [35]. The shift is greater for the S2 material ( $1.3\ 2\theta$ ), this being  $1.1\ 2\theta$  for the S1 sample (Figure S1). This may be due to the higher penetration of copper into the platinum lattice as a result of the staged synthesis. The average crystallite size determined by the Scherrer equation is 2.7 and 2.5 nm for the S1 and S2 samples, respectively.

The compositions, as determined by Vegard's law, for S1 and S2 are Pt<sub>65</sub>Cu<sub>35</sub> and Pt<sub>60</sub>Cu<sub>40</sub>, respectively. For sample S2, the XRD composition is close to that determined by XRF, while for S1, a reduced copper content is observed. Apparently, not all copper is

included in the composition of the NPs, and part of it is present on the surface in the form of X-ray amorphous oxide in S1.

The micrographs of the PtCu/C samples demonstrate the presence of the spherical, metal NPs distributed over the carbon support surface (Figure 1a,b,d,e). Based on the results of the TEM and HAADF-STEM studies, it may be concluded that there is the formation of a substantial number of agglomerates of more than 10 nm in size during the multistage synthesis of the S2 sample. Moreover, the less-uniform distribution of NPs over the support surface, as compared with the S1 material, is observed (Figure 1d,e). For the S1 material obtained in one stage, the proportion of agglomerates is significantly lower than that of the S2 sample (Figure 1a,b). A higher proportion of NPs in the S1 sample is made up of particles of a 4–6 nm size, these being 2–4 nm in the S2 material (Figure 1c,f).

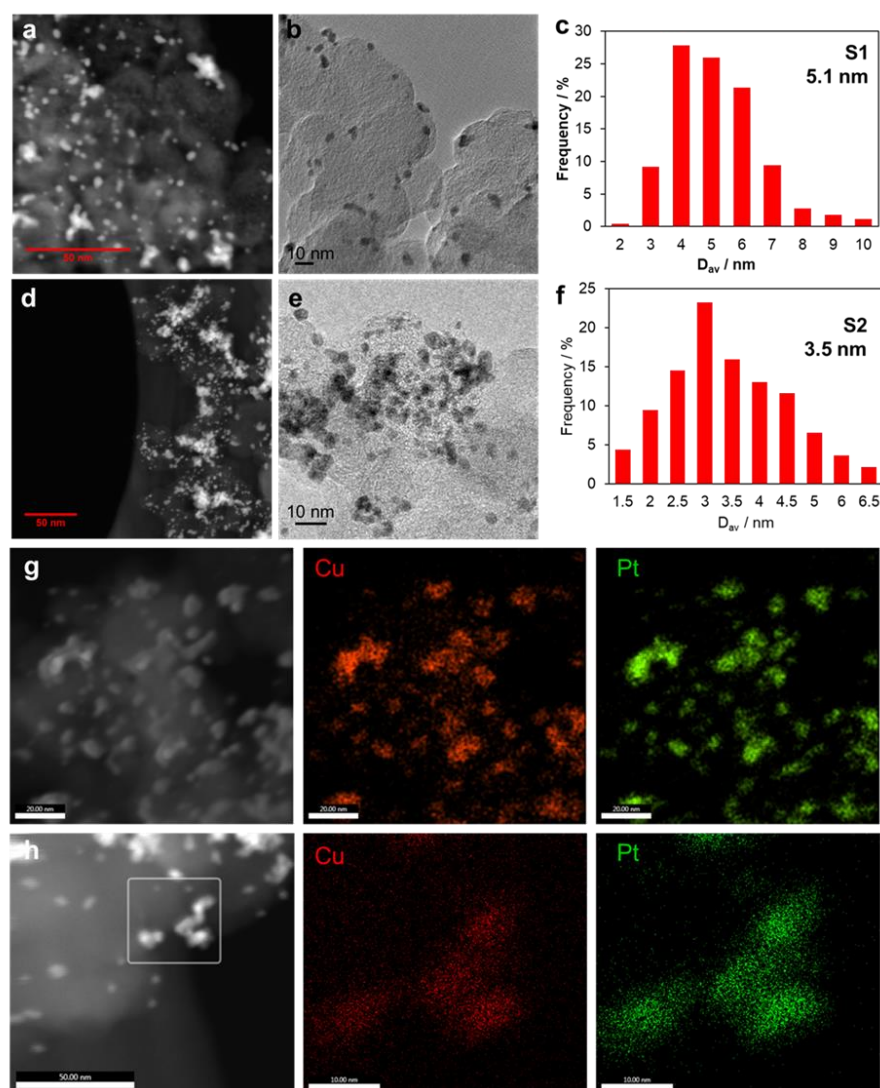


**Figure 1.** HAADF-STEM (a,d,g,h) and TEM (b,e) micrographs of the S1 (a,b,g) and S2 (d,e,h) samples; The NPs' size distribution in the corresponding materials (c,f); The elemental mapping of Cu and Pt in the presented area (g,h).

The elemental mapping of the obtained catalysts proves the localization of platinum and copper on the same sections of the support (Figure 1g,h). The atomic ratios of the metals as determined by the EDX method are  $Pt_{53}Cu_{47}$  and  $Pt_{68}Cu_{32}$  for the S1 and S2 samples, respectively.

As described in previous studies, a significant difference is observed in the ORR activity of PtCu/C materials activated in various potential ranges [18,32]. According to the procedures described in these studies, the catalysts were electrochemically activated by setting 100 voltametric cycles in the potential range of 0.04 to 1.0 V and of 0.04 to 1.2 V. Based on the protocol for electrochemical activation, the four activated materials are hereinafter referred to as S1<sub>1,2</sub>, S1<sub>1,0</sub>, S2<sub>1,2</sub>, and S2<sub>1,0</sub>.

The cyclic voltammograms (CVs) used to determine the ESA (Figure 2—ESA 0 black curves) and the linear sweep voltammograms (LSVs) to determine the ORR activity (Figure 3a,c,e,g—black curves) were registered after activation. The analysis of the metal component's composition after the electrochemical measurements is an additional method for estimating the changes taking place in the catalyst. The ADT consisted in the multiple repetition of the voltametric cycles (5K, 12 h), by the end of which, the CVs and the LSVs were registered.

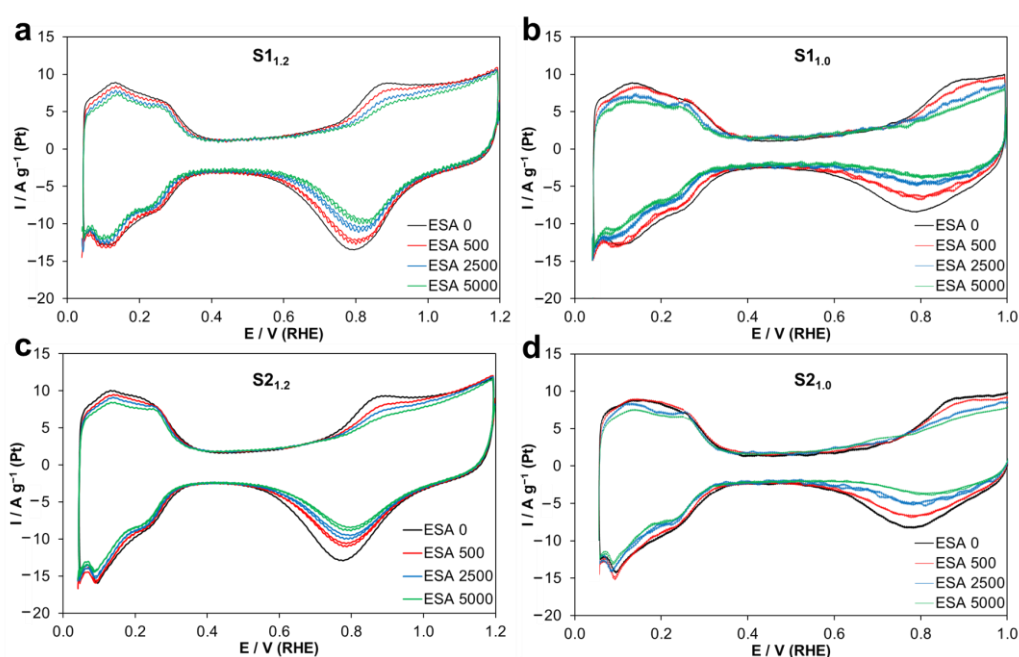


**Figure 2.** The CVs of the PtCu/C catalysts during different stages of the ADT. CVs are presented for materials S1<sub>1,2</sub> (a), S1<sub>1,0</sub> (b), S2<sub>1,2</sub> (c), and S2<sub>1,0</sub> (d).

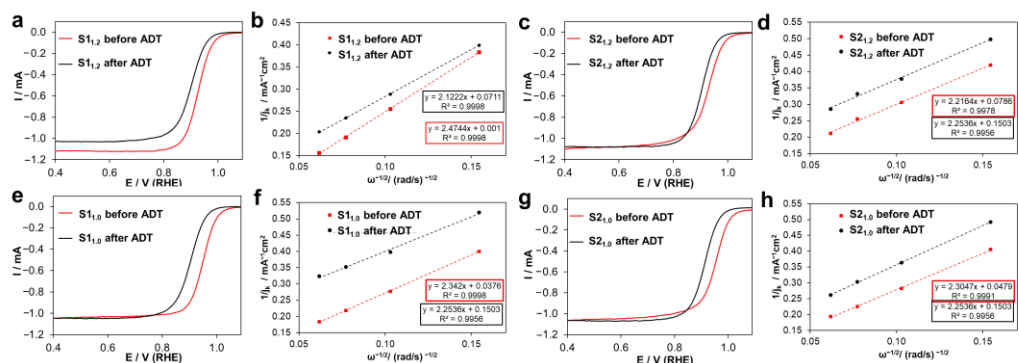


**Figure 3.** The ORR LSV curves of the PtCu/C catalysts before and after the ADT; the electrolyte is 0.1 M HClO<sub>4</sub>, under an O<sub>2</sub> atmosphere, 20 mV/s, 1600 rpm (a,c,e,g); The dependence in the Koutecky–Levich coordinates at 0.90 V (b,d,f,h) for the corresponding materials.

As previously described, the potential window of the activation has an ambiguous effect on the ESA values (Figure 3a) [18,32]. At the same time, the metals' atomic ratio as

determined by the results of the XRF is close to Pt<sub>70</sub>Cu<sub>30</sub> in each of the cases. The S2 sample is characterized by the higher initial ESA, as compared with the S1 material, regardless of the activation protocol. This correlates with the small size of the NPs (Figure 4). In this regard, the S<sub>2,1,2</sub> sample demonstrates the highest ESA, as compared with all of the materials studied.

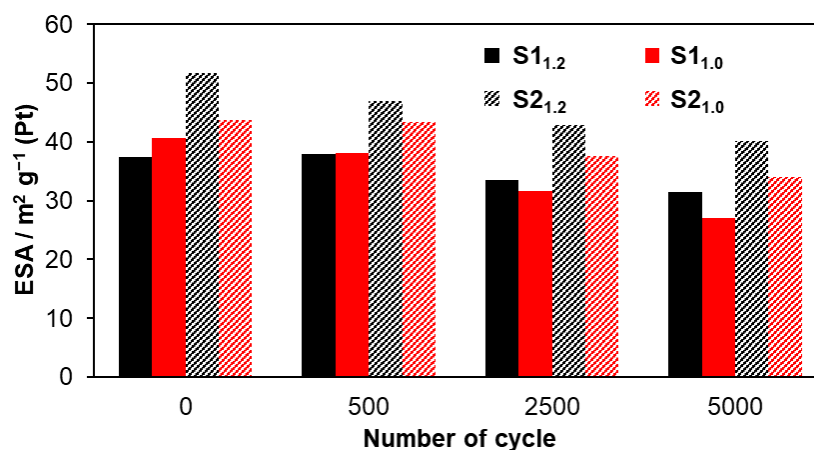


**Figure 4.** The ESA values of the PtCu/C catalysts during different stages of the ADT.

Since it is necessary to use the express method of stress testing to study the materials' durability under laboratory conditions, the protocol corresponding to the DOE standards, commonly used in different publications, was chosen [36–39]. The stress testing was conducted during 5000 cycles in the potential range of 0.6 to 1.0 V for all of the materials.

During the stress testing, the CVs were registered every 500, 1000, 2500, and 5000 cycles (Figure 4). The decrease in the currents in the hydrogen and oxygen regions is observed for all the PtCu/C materials throughout the ADT. This testifies to the decrease in the ESA and catalytic activity values (Figure 2). The greater the number of stress testing cycles imposed on a catalyst, the more pronounced the peaks of the adsorption/desorption of hydrogen (about 0.1 V and 0.25 V) will be. This indicates the rearrangement of the NPs' surface. The peaks of the formation/reduction of platinum oxide in the oxygen region (about 0.8–0.9 V) become less pronounced, which testifies to the degradation of the materials (Figure 2).

The histogram in Figure 4 demonstrates that the ESA changes equally for the S1 and S2 samples during all the stages of the study. As a result of the ADT, when activated to 1.2 V, both materials proved to obtain the higher residual ESA values, as compared with an activation to 1.0 V. The relative durability of the S<sub>1,1,2</sub> and S<sub>1,1,0</sub> materials as shown by the change in the ESA is 84% and 67%, respectively. These values for the S<sub>2,1,2</sub> and S<sub>2,1,0</sub> samples are 77% and 78%, respectively.

According to the results of the ADT, it may be concluded that the activation protocol has no significant effect on the relative durability of the S2 material with an onion-like structure of its NPs. When comparing the S<sub>1,1,0</sub> and S<sub>2,1,0</sub> materials, one can conclude that the sample with the onion-like structure of its NPs is more durable.

The ORR activity was registered before and after the ADT (Figure 2). The appearance of the current-voltage curves changes for all of the PtCu/C materials. The LSV curves are shifted to the region of lower potentials, and the E<sub>1/2</sub> decreases by 18, 42, 23, and 38 mV for the S<sub>1,1,2</sub>, S<sub>1,1,0</sub>, S<sub>2,1,2</sub>, and S<sub>2,1,0</sub> samples, respectively (Figure 3a,c,e,g). For the S<sub>1,1,2</sub> sample, the value of the limiting diffusion current largely decreases, as compared with the other PtCu/C materials (Figure 3a). This phenomenon may be caused by both the degradation processes and the mechanical detachment of a part of the catalyst from the end-face of the rotating disk electrode (RDE).

The kinetic current was calculated in regard to the dependence in the Koutetsky–Levich coordinates (Figure 3b,d,f,h). The ORR proceeds according to the 4-electron mechanism, which is typical for platinum, for all of the samples, both before and after the ADT.

The slope of the trend varies slightly for the S1<sub>1,2</sub> material, resulting in a decrease in the electrons' proportion from 3.8 to 3.5 after the ADT (Figure 3b). This is another descriptor of the degradation.

Regardless of the structure of the material, the potential window has a significant impact on the ORR activity of the catalysts (Figures 5 and S2), as previously described in reference [18]. As with the ESA, the relative decrease in the ORR activity is expected to be substantial for the S1<sub>1,0</sub> and S2<sub>1,0</sub> materials after the ADT (Figure 5 and Figure S2). The residual mass activity values after the ADT during the material's activation in the potential window from 0.04 to 1.0 V are 28% and 23% higher than those obtained during the activation in the potential window from 0.04 to 1.2 V for the S1 and S2 samples, respectively (Figures 5 and S2a). The change in the specific activity during the ADT is presented in Figure S2b.

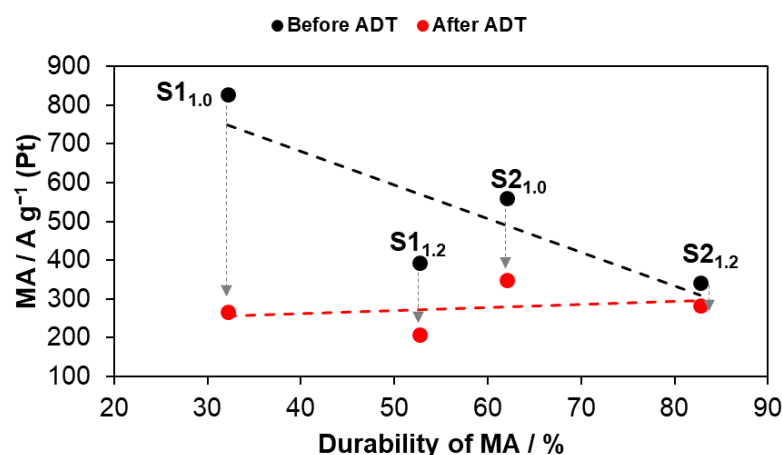


Figure 5. The dependence of the mass activity on the durability of the PtCu/C catalysts.

To facilitate a clear understanding of the changes taking place in the materials, the markers of the functional characteristics have been plotted on graphs of the dependence of the durability on the mass activity (Figure 5). The marker of the S1<sub>1,0</sub> sample in Figure 5 is characterized by the higher initial ORR activity and, at the same time, the greatest decrease of 600 A/g (Pt) in this parameter, which indicates significant degradation. The S2<sub>1,2</sub> sample, having the lowest activity values before the ADT, is characterized by a slight decrease of 50 A/g (Pt) in this parameter, which conforms to low degradation. Two extreme cases of this dependence have been considered herein.

The S1<sub>1,2</sub> and S2<sub>1,2</sub> samples are initially characterized by lower ORR activity due to the negative effect of the wider potential range during the activation stage [18,32]. Nevertheless, the S2<sub>1,2</sub> material proved to be more stable than the S1<sub>1,2</sub> material. This may be caused by the NPs' special architecture as obtained by the layered formation.

The catalyst which could maintain the higher ORR activity for a long time and, at the same time, exhibit a moderate value of durability (not lower than 50%) is assumed to be most promising. Therefore, the S2<sub>1,0</sub> sample is considered optimal in terms of the combination of the aforementioned parameters.

### 3. Materials and Methods

#### 3.1. The Synthesis of the PtCu/C Catalysts

The synthesis procedures of the studied materials are detailed in reference [18]. In summary, two PtCu/C materials were obtained via the single-stage (the S1 sample) and the multistage (the S2 sample) synthesis methods for solid-solution and onion-like structures of NPs, respectively, to be formed. The aqueous solutions of the metals' precursors (H<sub>2</sub>PtCl<sub>6</sub> and CuSO<sub>4</sub>) were used for the synthesis. The reduction was conducted in the liquid phase by excess sodium borohydride in an alkaline medium in the presence of carbon black

(Vulcan-XC72) with constant stirring. The obtained PtCu/C catalysts were filtered and dried over P<sub>2</sub>O<sub>5</sub> for 24 h.

### 3.2. The Study of the Catalysts' Structure

The structure of the catalysts was studied by the gravimetry, XRD, TXRF, TEM, HAADF-STEM, and EDX methods. The detailed description of these procedures is presented in the Supplementary Materials.

### 3.3. The Electrochemical Study of the Catalysts

To study the electrocatalysts, the cyclic voltammetry and linear sweep voltammetry methods in a standard three-electrode cell were used. The ESA was determined by the charge amount consumed for the adsorption/desorption of hydrogen. The data were extracted from the CV. The activity in the ORR was studied by the linear sweep voltammetry method on the RDE at different rotation speeds. The current values were established according to the dependence in the Koutetsky–Levich coordinates.

The ADT was conducted by cycling the catalyst for 5000 cycles in the potential range of 0.6 to 1.0 V.

The preparation procedure of the catalytic inks, as well as a detailed description of the electrochemical experiment, are presented in the Supplementary Materials.

## 4. Conclusions

The PtCu/C catalysts obtained by gram-scale synthesis methods were studied in this research. The applied techniques are facile in terms of their reproducibility and the equipment used. The obtained materials differ in the structure of the bimetallic NPs and exhibit higher ORR activity as compared with the DOE target (more than 440 A/g (Pt)). The staged method of the formation of the bimetallic NPs (the onion-like structure) results in optimal values for the ORR activity and durability during the ADT. The use of electrochemical activation in the potential range of 0.04 to 1.0 V was established so as to allow for an increase in the durability of the PtCu/C materials with different structures by an average of 25%, as compared with that produced by an activation in the potential range of 0.04 to 1.2 V.

Therefore, despite the non-homogeneity of the materials' morphology, the obtained bimetallic catalysts have proven to be highly active and stable during the ADT. At the same time, the choice of a potential window of 0.04 to 1.0 V allows for the achievement of higher residual characteristics. The combination of the high specific characteristics and a facile synthesis method opens up the prospects for the commercial production of the catalysts for PEMFCs.

**Supplementary Materials:** The following supporting information can be downloaded at: <https://www.mdpi.com/article/10.3390/inorganics11010045/s1>, Materials and methods of studying; Figure S1: XRD patterns of PtCu/C catalysts; Figure S2: The mass-activity (a) and specific activity (b) of the PtCu/C catalysts before and after the ADT.

**Author Contributions:** Conceptualization, A.P. and A.A.; investigation, A.P. and I.P.; writing—original draft preparation, A.P. and A.A.; writing—review and editing, A.P. and A.A. All authors have read and agreed to the published version of the manuscript.

**Funding:** This work was supported by the Ministry of Science and Higher Education of the Russian Federation (State Assignment in the Field of Scientific Activity No. 0852-2020-0019).

**Data Availability Statement:** Not applicable.

**Acknowledgments:** The authors are grateful to Nikulin A. Yu for assistance with the XRD pattern registration and to the Shared Use Center “High-Resolution Transmission Electron Microscopy” (SFedU) for conducting the TEM studies. The authors appreciate the support of LLC “PROMETHEUS R&D” (Rostov-on-Don) and LLC “Systems for Microscopy and Analysis” (Skolkovo, Moscow) for conducting the TEM and EDX studies. The authors are grateful to Maltsev A.V. for support with

translation and editing and assistance in communicating with the editorial board. We would like to acknowledge the Southern Federal University Strategic Academic Leadership Program (“Priority 2030”) for the support of the graduate students who took part in this study.

**Conflicts of Interest:** The authors declare no conflict of interest. The funders had no role in the design of the study; in the collection, analyses, or interpretation of data; in the writing of the manuscript; or in the decision to publish the results.

## References

1. Fan, J.; Chen, M.; Zhao, Z.; Zhang, Z.; Ye, S.; Xu, S.; Wang, H.; Li, H. Bridging the gap between highly active oxygen reduction reaction catalysts and effective catalyst layers for proton exchange membrane fuel cells. *Nat. Energy* **2021**, *6*, 475–486. [[CrossRef](#)]
2. Cruz-Martínez, H.; Rojas-Chávez, H.; Matadamas-Ortiz, P.; Ortiz-Herrera, J.; López-Chávez, E.; Solorza-Feria, O.; Medina, D. Current progress of Pt-based ORR electrocatalysts for PEMFCs: An integrated view combining theory and experiment. *Mater. Today Phys.* **2021**, *19*, 100406. [[CrossRef](#)]
3. Pollet, B.G.; Kocha, S.S.; Staffell, I. Current status of automotive fuel cells for sustainable transport. *Curr. Opin. Electrochem.* **2019**, *16*, 90–95. [[CrossRef](#)]
4. Guo, N.; Xue, H.; Bao, A.; Wang, Z.; Sun, J.; Song, T.; Ge, X.; Zhang, W.; Huang, K.; He, F.; et al. Achieving Superior Electrocatalytic Performance by Surface Copper Vacancy Defects during Electrochemical Etching Process. *Angew. Chem. Int. Ed.* **2020**, *59*, 13778–13784. [[CrossRef](#)] [[PubMed](#)]
5. Ercolano, G.; Farina, F.; Stievano, L.; Jones, D.J.; Rozière, J.; Cavaliere, S. Preparation of Ni@Pt core@shell conformal nanofibre oxygen reduction electrocatalysts via microwave-assisted galvanic displacement. *Catal. Sci. Technol.* **2019**, *9*, 6920–6928. [[CrossRef](#)]
6. Wang, D.; Xin, H.L.; Hovden, R.; Wang, H.; Yu, Y.; Muller, D.A.; Disalvo, F.J.; Abruña, H.D. Structurally ordered intermetallic platinum–cobalt core–shell nanoparticles with enhanced activity and stability as oxygen reduction electrocatalysts. *Nat. Mater.* **2013**, *12*, 81–87. [[CrossRef](#)]
7. Liu, L.; Liu, H.; Sun, X.; Li, C.; Bai, J. Efficient electrocatalyst of Pt–Fe/CNFs for oxygen reduction reaction in alkaline media. *Int. J. Hydrogen Energy* **2020**, *45*, 15112–15120. [[CrossRef](#)]
8. Sasaki, K.; Kuttiyiel, K.A.; Adzic, R.R. Designing high performance Pt monolayer core–shell electrocatalysts for fuel cells. *Curr. Opin. Electrochem.* **2020**, *21*, 368–375. [[CrossRef](#)]
9. Lyu, X.; Jia, Y.; Mao, X.; Li, D.; Li, G.; Zhuang, L.; Wang, X.; Yang, D.; Wang, Q.; Du, A.; et al. Gradient-Concentration Design of Stable Core–Shell Nanostructure for Acidic Oxygen Reduction Electrocatalysis. *Adv. Mater.* **2020**, *32*, e2003493. [[CrossRef](#)]
10. Alekseenko, A.A.; Guterman, V.E.; Belenov, S.V.; Menshikov, V.S.; Tabachkova, N.Y.; Safronenko, O.I.; Moguchikh, E.A. Pt/C electrocatalysts based on the nanoparticles with the gradient structure. *Int. J. Hydrogen Energy* **2018**, *43*, 3676–3687. [[CrossRef](#)]
11. Wu, J.; Gross, A.; Yang, H. Shape and Composition-Controlled Platinum Alloy Nanocrystals Using Carbon Monoxide as Reducing Agent. *Nano Lett.* **2011**, *11*, 798–802. [[CrossRef](#)]
12. Bu, L.; Guo, S.; Zhang, X.; Shen, X.; Su, D.; Lu, G.; Zhu, X.; Yao, J.; Guo, J.; Huang, X. Surface engineering of hierarchical platinum–cobalt nanowires for efficient electrocatalysis. *Nat. Commun.* **2016**, *7*, 11850. [[CrossRef](#)]
13. Pavlets, A.; Alekseenko, A.; Tabachkova, N.Y.; Safronenko, O.; Nikulin, A.Y.; Alekseenko, D.; Guterman, V. A novel strategy for the synthesis of Pt–Cu uneven nanoparticles as an efficient electrocatalyst toward oxygen reduction. *Int. J. Hydrogen Energy* **2021**, *46*, 5355–5368. [[CrossRef](#)]
14. Cai, X.; Lin, R.; Shen, D.; Zhu, Y. Gram-Scale Synthesis of Well-Dispersed Shape-Controlled Pt–Ni/C as High-Performance Catalysts for the Oxygen Reduction Reaction. *ACS Appl. Mater. Interfaces* **2019**, *11*, 29689–29697. [[CrossRef](#)]
15. Hu, B.; Yuan, J.; Zhang, J.; Shu, Q.; Guan, D.; Yang, G.; Zhou, W.; Shao, Z. High activity and durability of a Pt–Cu–Co ternary alloy electrocatalyst and its large-scale preparation for practical proton exchange membrane fuel cells. *Compos. Part B Eng.* **2021**, *222*, 109082. [[CrossRef](#)]
16. Moriau, L.J.; Hrnjić, A.; Pavličič, A.; Kamšek, A.R.; Petek, U.; Ruiz-Zepeda, F.; Šala, M.; Pavko, L.; Šelih, V.S.; Bele, M.; et al. Resolving the nanoparticles’ structure-property relationships at the atomic level: A study of Pt-based electrocatalysts. *IScience* **2021**, *24*, 102102. [[CrossRef](#)]
17. Jovanović, P.; Šelih, V.S.; Šala, M.; Hočevar, S.B.; Pavličič, A.; Gatalo, M.; Bele, M.; Ruiz-Zepeda, F.; Čekada, M.; Hodnik, N.; et al. Electrochemical in-situ dissolution study of structurally ordered, disordered and gold doped PtCu<sub>3</sub> nanoparticles on carbon composites. *J. Power Sources* **2016**, *327*, 675–680. [[CrossRef](#)]
18. Alekseenko, A.; Pavlets, A.; Belenov, S.; Safronenko, O.; Pankov, I.; Guterman, V. The electrochemical activation mode as a way to exceptional ORR performance of nanostructured PtCu/C materials. *Appl. Surf. Sci.* **2022**, *595*, 153533. [[CrossRef](#)]
19. Pavlets, A.; Alekseenko, A.; Nikolskiy, A.; Kozakov, A.; Safronenko, O.; Pankov, I.; Guterman, V. Effect of the PtCu/C electrocatalysts initial composition on their activity in the de-alloyed state in the oxygen reduction reaction. *Int. J. Hydrogen Energy* **2022**, *47*, 30460–30471. [[CrossRef](#)]
20. Wang, D.; Yu, Y.; Xin, H.L.; Hovden, R.; Ercius, P.; Mundy, J.A.; Chen, H.; Richard, J.H.; Muller, D.A.; DiSalvo, F.J.; et al. Tuning Oxygen Reduction Reaction Activity via Controllable Dealloying: A Model Study of Ordered Cu<sub>3</sub>Pt/C Intermetallic Nanocatalysts. *Nano Lett.* **2012**, *12*, 5230–5238. [[CrossRef](#)]

21. Belenov, S.; Alekseenko, A.; Pavlets, A.; Nevelskaya, A.; Danilenko, M. Architecture Evolution of Different Nanoparticles Types: Relationship between the Structure and Functional Properties of Catalysts for PEMFC. *Catalysts* **2022**, *12*, 638. [CrossRef]
22. Jung, J.Y.; Kim, D.-G.; Jang, I.; Kim, N.D.; Yoo, S.J.; Kim, P. Synthesis of hollow structured PtNi/Pt core/shell and Pt-only nanoparticles via galvanic displacement and selective etching for efficient oxygen reduction reaction. *J. Ind. Eng. Chem.* **2022**, *111*, 300–307. [CrossRef]
23. Gatalo, M.; Moriau, L.; Petek, U.; Ruiz-Zepeda, F.; Šala, M.; Grom, M.; Galun, T.; Jovanovič, P.; Pavlišič, A.; Bele, M.; et al. CO-assisted ex-situ chemical activation of Pt-Cu/C oxygen reduction reaction electrocatalyst. *Electrochimica Acta* **2019**, *306*, 377–386. [CrossRef]
24. Menshchikov, V.; Alekseenko, A.; Guterman, V.; Nechitailov, A.; Glebova, N.; Tomasov, A.; Spiridonova, O.; Belenov, S.; Zelenina, N.; Safronenko, O. Effective Platinum-Copper Catalysts for Methanol Oxidation and Oxygen Reduction in Proton-Exchange Membrane Fuel Cell. *Nanomaterials* **2020**, *10*, 742. [CrossRef]
25. Wang, D.; Yu, Y.; Zhu, J.; Liu, S.; Muller, D.A.; Abruña, H.D. Morphology and Activity Tuning of Cu<sub>3</sub>Pt/C Ordered Intermetallic Nanoparticles by Selective Electrochemical Dealloying. *Nano Lett.* **2015**, *15*, 1343–1348. [CrossRef]
26. Gatalo, M.; Jovanovic, P.; Ruiz-Zepeda, F.; Pavlišič, A.; Robba, A.; Bale, M.; Dražič, G.; Gaberšček, M.; Hodnik, N. Insights into electrochemical dealloying of Cu out of Au-doped Pt-alloy nanoparticles at the sub-nano-scale. *J. Electrochem. Sci. Eng.* **2018**, *8*, 87–100. [CrossRef]
27. Barim, S.B.; Bozbag, S.E.; Deljoo, B.; Aindow, M.; Erkey, C. Highly Active Carbon Supported PtCu Electrocatalysts for PEMFCs by in situ Supercritical Deposition Coupled with Electrochemical Dealloying. *Fuel Cells* **2019**, *20*, 285–299. [CrossRef]
28. Yang, T.; Pukazhselvan, D.; da Silva, E.; Santos, M.C.; Meng, L.; Ramasamy, D.; Jothi, S.; Graca, V.; Shi, S. Highly branched Pt Cu nanodandelion with high activity for oxygen reduction reaction. *Int. J. Hydrogen Energy* **2018**, *44*, 174–179. [CrossRef]
29. Pizzutilo, E.; Geiger, S.; Grote, J.-P.; Mingers, A.; Mayrhofer, K.J.J.; Arenz, M.; Cherevko, S. On the Need of Improved Accelerated Degradation Protocols (ADPs): Examination of Platinum Dissolution and Carbon Corrosion in Half-Cell Tests. *J. Electrochem. Soc.* **2016**, *163*, F1510–F1514. [CrossRef]
30. Impagnatiello, A.; Cerqueira, C.F.; Coulon, P.-E.; Morin, A.; Escribano, S.; Guétaz, L.; Clochard, M.-C.; Rizza, G. Degradation Mechanisms of Supported Pt Nanocatalysts in Proton Exchange Membrane Fuel Cells: An Operando Study through Liquid Cell Transmission Electron Microscopy. *ACS Appl. Energy Mater.* **2020**, *3*, 2360–2371. [CrossRef]
31. Khalakhan, I.; Waidhas, F.; Brummel, O.; Vorokhta, M.; Kúš, P.; Yakovlev, Y.V.; Bertram, M.; Dopita, M.; Matolínová, I.; Libuda, J.; et al. Nanoscale Morphological and Structural Transformations of PtCu Alloy Electrocatalysts during Potentiodynamic Cycling. *J. Phys. Chem. C* **2018**, *122*, 21974–21982. [CrossRef]
32. Pavlets, A.; Alekseenko, A.; Menshchikov, V.; Belenov, S.; Volochaev, V.; Pankov, I.; Safronenko, O.; Guterman, V. Influence of Electrochemical Pretreatment Conditions of PtCu/C Alloy Electrocatalyst on Its Activity. *Nanomaterials* **2021**, *11*, 1499. [CrossRef]
33. Ghavidel, M.R.Z.; Monteverde Videla, A.H.A.; Specchia, S.; Easton, E.B. The relationship between the structure and ethanol oxidation activity of Pt-Cu/C alloy catalysts. *Electrochim. Acta* **2017**, *230*, 58–72. [CrossRef]
34. Liao, Y.; Wang, Y.; Liu, J.; Tang, Y.; Wu, C.; Chen, Y. Ordered Mesoporous Carbon Confined Highly Dispersed PtCo Alloy for the Oxygen Reduction Reaction: The Effect of Structure and Composition on Performance. *Ind. Eng. Chem. Res.* **2021**, *60*, 14728–14736. [CrossRef]
35. Pryadchenko, V.V.; Srabionyan, V.V.; Kurzin, A.A.; Bulat, N.V.; Shemet, D.B.; Avakyan, L.A.; Belenov, S.V.; Volochaev, V.A.; Zizak, I.; Guterman, V.E.; et al. Bimetallic PtCu core-shell nanoparticles in PtCu/C electrocatalysts: Structural and electrochemical characterization. *Appl. Catal. A Gen.* **2016**, *525*, 226–236. [CrossRef]
36. DOE Durability Working Group. Rotating Disk-Electrode Aqueous Electrolyte Accelerated Stress Tests for PGM Electrocatalyst/Support Durability Evaluation. Available online: [https://www.energy.gov/sites/prod/files/2015/08/f25/fcto\\_dwg\\_pgm\\_electrocatalyst\\_support\\_aqueous\\_ast.pdf](https://www.energy.gov/sites/prod/files/2015/08/f25/fcto_dwg_pgm_electrocatalyst_support_aqueous_ast.pdf) (accessed on 25 December 2022).
37. Zhu, H.; Cai, Y.; Wang, F.; Gao, P.; Cao, J. Scalable Preparation of the Chemically Ordered Pt–Fe–Au Nanocatalysts with High Catalytic Reactivity and Stability for Oxygen Reduction Reactions. *ACS Appl. Mater. Interfaces* **2018**, *10*, 22156–22166. [CrossRef]
38. Stariha, S.; Macauley, N.; Sneed, B.T.; Langlois, D.; More, K.L.; Mukundan, R.; Borup, R.L. Recent Advances in Catalyst Accelerated Stress Tests for Polymer Electrolyte Membrane Fuel Cells. *J. Electrochem. Soc.* **2018**, *165*, F492–F501. [CrossRef]
39. Chen, Z.; Liao, Y.; Chen, S. Facile synthesis of platinum-copper aerogels for the oxygen reduction reaction. *Energy Mater.* **2022**, *2*, 200033. [CrossRef]

**Disclaimer/Publisher’s Note:** The statements, opinions and data contained in all publications are solely those of the individual author(s) and contributor(s) and not of MDPI and/or the editor(s). MDPI and/or the editor(s) disclaim responsibility for any injury to people or property resulting from any ideas, methods, instructions or products referred to in the content.